

Thermodynamics of the Spin Luttinger Liquid in a Model Ladder Material

Ch. Rüegg,¹ K. Kiefer,² B. Thielemann,³ D. F. McMorrow,¹ V. Zapf,⁴ B. Normand,⁵ M. B. Zvonarev,⁶ P. Bouillot,⁶ C. Kollath,⁷ T. Giamarchi,⁶ S. Capponi,^{8,9} D. Poilblanc,^{9,8} D. Biner,¹⁰ and K. W. Krämer¹⁰

¹London Centre for Nanotechnology; University College London; London WC1E 6BT; United Kingdom

²BENS; Helmholtz Centre Berlin for Materials and Energy; D-14109 Berlin; Germany

³Laboratory for Neutron Scattering; ETH Zurich and Paul Scherrer Institute; CH-5232 Villigen PSI; Switzerland

⁴NHMFL; Los Alamos National Laboratory; Los Alamos; New Mexico 87545; USA

⁵Institute for Theoretical Physics; Ecole Polytechnique Fédérale de Lausanne; CH-1015 Lausanne; Switzerland

⁶DPMC-MaNEP; Université de Genève; CH-1211 Geneva 4; Switzerland

⁷Centre de Physique Théorique; École Polytechnique; CNRS; 91128 Palaiseau; France

⁸Université de Toulouse; UPS; Laboratoire de Physique Théorique; IRSAMC; F-31062 Toulouse; France

⁹CNRS; UMR 5152; F-31062 Toulouse; France

¹⁰Department of Chemistry and Biochemistry; University of Bern; CH-3000 Bern 9; Switzerland

(Dated: February 20, 2024)

The phase diagram in temperature and magnetic field of the metal-organic, two-leg, spin-ladder compound $(\text{C}_5\text{H}_{12}\text{N})_2\text{CuBr}_4$ is studied by measurements of the specific heat and the magnetocaloric effect. We demonstrate the presence of an extended spin Luttinger-liquid phase between two field-induced quantum critical points and over a broad range of temperature. Based on an ideal spin-ladder Hamiltonian, comprehensive numerical modelling of the ladder specific heat yields excellent quantitative agreement with the experimental data across the complete phase diagram.

PACS numbers: 75.10.Jm; 75.40.Cx; 75.40.Mg

Quantum spin systems display a remarkable diversity of fascinating physical behavior. This is especially true for systems such as spin ladders, which have a gapped or a gapless ground state, respectively, for an even or an odd number of ladder legs [1]. For two-leg ladders, and in general for any even leg number, quantum phase transitions (QPTs) between gapped and gapless phases can be driven by an external magnetic field. While these QPTs are generic in quantum magnets [2], the nature of the gapless phase depends crucially on the dimensionality of the spin system. In two and higher dimensions, a quantum critical point (QCP) separates the low-field, quantum disordered (QD) phase, with gapped triplet excitations, from a gapless phase with long-range antiferromagnetic (AF) order, which can be well described as a Bose-Einstein Condensate (BEC) of magnons [2, 3, 4].

By contrast, for one-dimensional (1D) systems such as ladders, both long-ranged magnetic order and BEC are precluded due to phase fluctuations. In addition, spin excitations are best viewed as interacting fermions, whereas a bosonic representation pertains in higher dimensions. The physics of the gapless phase in 1D is thus quite different. It is a (spin) Luttinger liquid (LL) [5], and is a key component of the rich phase diagram presented in Fig. 1 [3, 6, 7, 8, 9]. In the LL, the spectrum is gapless with algebraically decaying spin correlations. Because there is no finite order parameter, the LL regime is reached from the high-temperature, classical regime through a crossover rather than a phase transition. Nevertheless, clear manifestations of LL behavior are expected not only in the correlation functions but also in thermodynamic quantities such as the magnetization and specific heat.

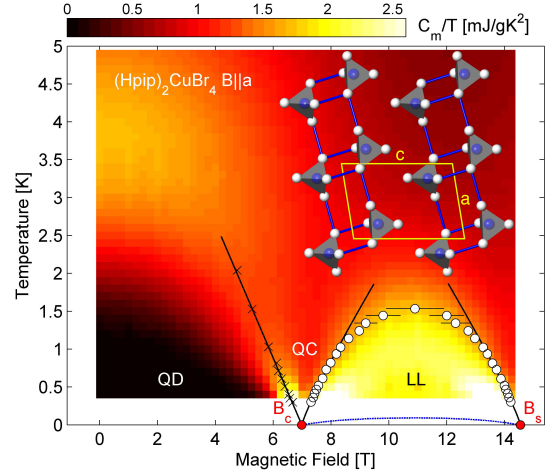


FIG. 1: Field-temperature phase diagram of the spin-ladder compound $(\text{Hpip})_2\text{CuBr}_4$, showing quantum disordered (QD), quantum critical (QC), and spin Luttinger liquid (LL) phases. QCPs occur at B_c (closing of spin triplet gap Δ) and B_s (spin system fully polarized). The contour plot shows the magnetic specific heat as $C_m(T, B)/T$. Local maxima from the reduction of the triplet gap by the Zeeman effect are indicated by crosses. Circles denote the LL crossover based on measurements of the magnetocaloric effect [Fig. 4], black lines are fits to extract the critical fields, and the dashed blue line indicates the onset of long-ranged order below 100 mK [21, 22]. Inset: lattice structure of $(\text{Hpip})_2\text{CuBr}_4$ in projection along the b -axis, with Cu atoms blue and Br white.

However, materials in which to explore such effects are rather rare. Investigations of the spin excitations and

thermodynamic properties of ladder compounds have to date been performed primarily on copper oxides. In these materials, the exchange interactions are typically some hundreds of meV, and thus the phases are not easily controlled by a magnetic field. Candidate 1D materials in which thermodynamic properties have been studied around the QPT include the bond-alternating $S = 1/2$ and $S = 1$ chains F_5PNN [10] and NTEMP [11], the $S = 1$ Haldane system NDMAP [12, 13], and the $S = 1/2$ system CuHpCl [14], which was for some time considered to be a spin ladder [15]. While measurements in these materials show indications of LL behavior in parts of the field–temperature phase diagram, their magnetic properties are influenced in large part by the presence of significant single-ion anisotropy and/or three-dimensional (3D) interactions between the chains, which tend to dominate the low-temperature specific heat at all fields [16]. Hence we have pursued the search for materials suitable to study the intrinsic spin LL physics by seeking those showing, at minimum, a clear separation of energy (temperature) scales between 1D and 3D interactions.

Here we present the results of thermodynamic measurements on an exceptional two-leg ladder material, the compound piperidinium copper bromide $(\text{C}_5\text{H}_{12}\text{N})_2\text{CuBr}_4$ [17, 18, 19, 20, 21, 22], where all of the phases of interest can be accessed, as summarized in Fig. 1. In particular, we find an extended region in the phase diagram, between 0.1 K and 1.5 K, where a spin LL is observed. We show that the crossover into the LL is signaled by clear features in both the specific heat and the magnetization. In the gapless spin LL, the magnetic specific heat is linear at low temperatures. Its field- and temperature-dependence are in excellent agreement with numerical calculations involving no free parameters. This demonstrates that the material is very accurately described by a minimal spin-ladder Hamiltonian.

High-quality single crystals of $(\text{C}_5\text{H}_{12}\text{N})_2\text{CuBr}_4$, abbreviated $(\text{Hpip})_2\text{CuBr}_4$ in the following, were grown from solution. In this material, the $S = 1/2$ magnetic moments of the Cu^{2+} ions are arranged in a ladder-like structure along the a -axis [Fig. 1, inset]. The rungs (J_r) of this ladder are formed by two equivalent $\text{Cu}-\text{Br}-\text{Br}-\text{Cu}$ superexchange paths with a center of inversion symmetry [16], while the legs (J_l) involve one similar but longer interaction path. The ladder units $(\text{Cu}_2\text{Br}_8)^{4-}$ are well separated by the organic $(\text{C}_5\text{H}_{12}\text{N})^+$ cations, which contribute only very little to the electronic properties of the host structure, and hence any magnetic exchange between ladders (J') is expected to be small. Direct measurements of these interactions, $J_r=12.9(2)$ K, $J_l=3.3(3)$ K, and $J' < 100$ mK, based on inelastic neutron scattering experiments [23], are in very close agreement with the values extracted from magnetostriction [20] and nuclear magnetic resonance (NMR) [21] measurements.

The specific heat and magnetocaloric effect (MCE) were measured on a purpose-built calorimeter at the

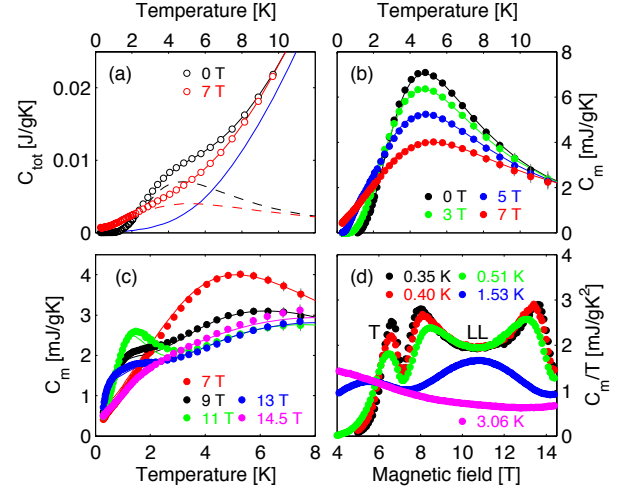


FIG. 2: (a) Measured total specific heat $C_{\text{tot}}(T)$ at fixed magnetic field. Solid (dashed) lines are based on fits to the data before (after) background subtraction. The blue line indicates the uniform, non-magnetic background. (b) Magnetic specific heat $C_m(T, B)$ for $B \leq B_c$, and (c) $B_c \leq B \leq B_s$. Lines in (a–c) show C_m^{ED} , and are based on ED and DMRG calculations, as explained in the text. (d) $C_m(T, B)/T$ measured at fixed temperature. The region with linear temperature-dependence of the specific heat is indicated by LL, while T marks the peak due to the softening triplet.

Helmholtz Centre Berlin (Laboratory for Magnetic Measurements at BENSCH), using single crystals of masses 4.78 mg and 9.69 mg in the respective temperature and field ranges 0.3 K to 15 K and 0 T to 14.5 T. The field was applied parallel to the crystallographic a -axis, a geometry in which we obtained the values $B_c = 6.99(5)$ T and $B_s = 14.4(1)$ T for the two QCPs [Fig. 1]. The specific heat was extracted from a quasi-adiabatic relaxation technique and, using the same set-up, the MCE was recorded with a sweep rate of 0.05 T per minute.

In Fig. 1 the magnetic component of the specific heat C_m/T of $(\text{Hpip})_2\text{CuBr}_4$ is presented across the entire phase diagram. It shows clearly three distinct regimes: QD, quantum critical (QC), and spin LL. The contour plot was obtained from 27 scans in field and temperature, after subtraction of a field-independent lattice contribution $C_l(T)$ and of a small nuclear term, which both are determined from a simultaneous fit to all available data.

In Fig. 2 (a)–(d) we show individual measurements of the total and the magnetic specific heat, respectively $C_{\text{tot}}(T)$ and $C_m(T, B)$. In the QD regime, $B \leq B_c$, C_m shows a single peak at approximately 5 K [Fig. 2(b)]. This peak is attributable to the triplet excitations of the ladder, and is exponentially activated at lower temperatures due to the presence of the spin gap Δ [24]. With increasing field, the gap is reduced by the Zeeman effect ($\Delta \rightarrow \Delta - g\mu_B B$). Field scans such as those in Fig. 2(d) show most clearly the reduction of the gap and are used

to extract the critical field B_c in Fig. 1, yielding very good agreement with determinations by complementary experimental techniques [18, 19, 20, 21, 22].

The specific heat changes dramatically for fields $B > B_c$, which we explain by the formation of the LL phase [Fig. 2(c)]. While at high temperature C_m is dominated by the (gapped) $S_z = 0$ triplet states, at low temperature an additional peak develops. Below this peak, the temperature-dependence remains linear up to $B = B_s \approx 14.5$ T, with a field-dependent slope. The linearity of C_m is demonstrated in Fig. 2(d). For fields near the maximum of the LL dome, the ratio C_m/T measured at different temperatures collapses onto the same curve. This temperature-dependence is consistent with the presence of gapless spinon excitations with a finite velocity u , its slope being inversely proportional to u [5]. The first peak thus occurs when the temperature is large enough to probe deviations from this linear regime. It can be taken as an estimate of the crossover to enter the LL, and is visible in Fig. 1 for $B_c < B < B_s$. The field-dependence of C_m is almost symmetric about $(B_c + B_s)/2 \approx 10.7$ T. In the strong-coupling limit, $J_r/J_l \gg 1$, a perfect symmetry would be expected due to the exact particle-hole symmetry of the XXZ chain in a field [14, 25]. Here we observe clearly deviations characteristic of the underlying ladder structure. Similar effects are also visible in spin correlation functions and in the low-temperature phase diagram, which can be measured by NMR [21] and neutron scattering [22].

At $B > B_s$, the specific heat becomes exponentially activated again due to the opening of a field-dependent spin gap in the fully saturated phase. However, this regime is close to the limit of our experimental window, and so the high-field phase is not investigated further here.

The experimental data have been compared with several theoretical calculations, and the agreement is remarkable (Fig. 2). Numerical results were obtained by exact diagonalization (ED) and by adaptive, time-dependent density-matrix renormalization-group (DMRG) calculations [26], both performed for a single ladder with $J_r=13$ K, $J_r/J_l=4$, and $g=2.06$ (*i.e.* no free parameters). We stress that in both techniques it is important to retain a sufficient number of ladder states for a quantitative description of thermodynamic data. The DMRG calculations (2×40 spins) may be regarded as the definitive behavior of this model. In the ED calculations, the specific heat of even- (odd-)length ladders converges rapidly from above (below) to the infinite-size limit; thus finite-size effects are essentially removed here by taking an average between systems of 2×10 and 2×11 spins. The ED and DMRG results are indistinguishable both in the QD phase [Fig. 2(b)] and in the LL regime [Fig. 2(c)]. Slight deviations from the experimental data are found only close to the upper critical field B_s and at 11 T.

Some physical insight into the numerical results is afforded by two approximate treatments. A statisti-

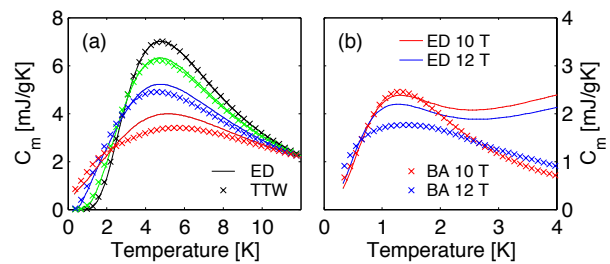


FIG. 3: Comparison of calculated ladder specific heat. (a) ED vs. TTW for magnetic-field values $B \leq B_c$ [Fig. 2(b)]. (b) ED vs. BA for some magnetic-field values $B > B_c$ [Fig. 2(c)].

cal Ansatz (TTW) [24] developed for spin ladders, and shown previously to describe very accurately the thermal renormalization of triplet excitations in the 3D dimer system TiCuCl_3 [27], uses the correct number of states but applies their hard-core constraint only globally. In the spin ladder, this approximation underestimates the local energy of the excited states, leading to a systematic shift of weight to lower energies as $B \rightarrow B_c$ [Fig. 3(a)]. A mapping of the lowest two modes of the ladder Hamiltonian onto an effective $S = 1/2$ XXZ chain [14, 25], whence thermodynamic quantities are computed exactly from the Bethe Ansatz (BA), is very accurate for the low-energy physics at $B > B_c$, but cannot reproduce the heat capacity at higher temperatures because of the missing triplet states ($S_z = 0, -1$) [Fig. 3(b)]. We conclude that the thermodynamic properties of $(\text{Hpip})_2\text{CuBr}_4$ are described very accurately by a model of a single two-leg ladder, and that comprehensive measurements of the specific heat identify an extended LL regime.

We turn now to a different observable, the uniform magnetization (M), which is notoriously difficult to measure at temperatures below 1.5 K. Very precise measurements can be obtained by NMR [21], but here we use an alternative method to probe the crossover to the LL. We determine the derivative of the magnetization with respect to temperature using the relation $(\delta Q/\delta B)/T = -(\partial M/\partial T)|_B$, where δQ is the amount of heat created or absorbed by the sample for a field change δB due to the MCE. Figure 4 shows both representative $(\delta Q/\delta B)/T$ -traces (corrected for a small base-line drift at higher temperatures) and a contour plot of all available data, presenting directly $\partial M/\partial T$. In the free-fermion model, which is an excellent qualitative description of spins near the QCP in 1D [5], and in more refined approaches [8, 9, 29], the magnetization presents a minimum or maximum as a function of temperature ($\partial M/\partial T = 0$). These extrema occur when the temperature matches the chemical potential, and thus provide another determination of the crossover temperature for the LL phase. The extracted phase boundary and the positions of the peaks in the specific heat agree well within expectations, as

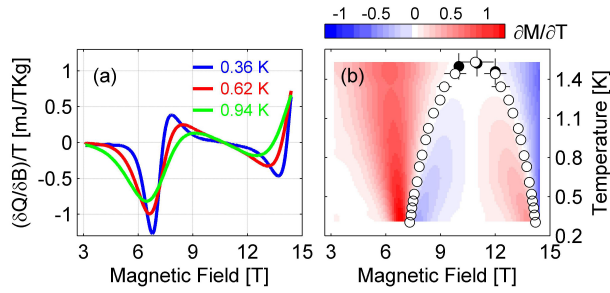


FIG. 4: Magnetocaloric effect in $(\text{Hpip})_2\text{CuBr}_4$. (a) Heat-flow δQ to and from the sample as a function of magnetic field divided by temperature, $(\delta Q/\delta B)/T$. (b) Contour plot of $\partial M/\partial T$ as a function of field and temperature. White circles denote the phase boundary derived from $\partial M/\partial T = 0$ (see also Fig. 1), while black circles are maxima in the specific heat, $\partial C_m/\partial T = 0$, obtained at fixed field.

demonstrated by the solid symbols in Fig. 4(b).

The structures present here in the magnetization and specific heat differ markedly from those occurring when there is a BEC. In that case, because a real phase transition occurs, the specific heat diverges with a λ -type anomaly. Such a shape has been observed at BEC transitions in higher-dimensional materials such as $\text{BaCuSi}_2\text{O}_6$ [28]. At the same temperature the magnetization develops a minimum, but with a cusp-like structure [3], which has been observed in TiCuCl_3 [4]. For 1D spin ladders, the magnetization minimum and the specific-heat peak have a different origin: they correspond to the crossover to the LL regime. Thus there is no divergence in the specific heat and the magnetization minimum is analytic, reflecting the absence of a phase transition; the temperatures of the two features, although similar, are not identical. For $(\text{Hpip})_2\text{CuBr}_4$, a real phase transition of BEC type does occur at a much lower temperature, $T_N \approx 100$ mK (Fig. 1, [21, 22]), due to a 3D coupling of the ladders.

In summary, we have measured the specific heat and magnetocaloric effect in the metal-organic, two-leg spin ladder $(\text{C}_5\text{H}_{12}\text{N})_2\text{CuBr}_4$. The excellent low-dimensionality and optimal energy scale of the exchange interactions make this material unique, and allow a detailed investigation of the phase diagram in temperature and in fields up to magnetic saturation for the quantum spin ladder. We find an extended region of spin Luttinger liquid behavior over at least one order of magnitude in temperature, lying clearly above any three-dimensional physics triggered by residual interladder interactions. The high-precision experimental data have been analyzed using the most advanced exact diagonalization and density matrix renormalization group techniques to calculate thermodynamic quantities for all of the phases (*i.e.* across two quantum critical points). From the direct and parameter-free fit of the experimental and numerical results, we conclude that $(\text{C}_5\text{H}_{12}\text{N})_2\text{CuBr}_4$ is re-

markably well described by a minimal spin-ladder Hamiltonian, with other possible effects (frustrated interactions, Dzyaloshinskii-Moriya terms, lattice coupling) being very small. Hence the material offers unprecedented opportunities to investigate the intrinsic physics of low-dimensional quantum systems.

We are grateful to C. Berthier and F. Essler for helpful discussions. This work was supported by the Royal Society, EPSRC, the Wolfson Foundation, the network 'Triangle de la Physique', the Swiss National Science Foundation through the NCCR MaNEP and Division II, and the French National Council (ANR). S.C. thanks Calmip (Toulouse) for computing time.

-
- [1] E. Dagotto and T. M. Rice, *Science* **271**, 618 (1996).
 - [2] T. Giamarchi, Ch. Rüegg, and O. Tchernyshyov, *Nature Physics* **4**, 198 (2008).
 - [3] T. Giamarchi and A. M. Tsvelik, *Phys. Rev. B* **59**, 11398 (1999).
 - [4] T. Nikuni and M. Oshikawa and A. Oosawa and H. Tanaka, *Phys. Rev. Lett.* **84**, 5868 (2000).
 - [5] T. Giamarchi, *Quantum Physics in One Dimension*, Oxford University Press, 2004.
 - [6] S. Sachdev, T. Senthil, and R. Shankar, *Phys. Rev. B* **50**, 258 (1994).
 - [7] A. Furusaki and S. C. Zhang, *Phys. Rev. B* **60**, 1175 (1999).
 - [8] X. Wang and L. Yu, *Phys. Rev. Lett.* **84**, 5399 (2000).
 - [9] S. Wessel, M. Olshanii, and S. Haas, *Phys. Rev. Lett.* **87**, 206407 (2001).
 - [10] Y. Yoshida *et al.*, *Phys. Rev. Lett.* **94**, 037203 (2005).
 - [11] M. Hagiwara *et al.*, *Phys. Rev. Lett.* **96**, 147203 (2006).
 - [12] Z. Honda, K. Katsumata, Y. Nishiyama, and I. Harada, *Phys. Rev. B* **63**, 064420 (2001).
 - [13] Y. Shen *et al.*, *Phys. Rev. Lett.* **86**, 1618 (2001).
 - [14] G. Chaboussant *et al.*, *Eur. Phys. J. B* **6**, 167 (1998).
 - [15] M.B. Stone *et al.*, *Phys. Rev. B* **65**, 064423 (2002).
 - [16] In the absence of inversion symmetry, as in CuHfCl , also Dzyaloshinskii-Moriya interactions can play an important role. See *e.g.* S. Capponi and D. Poilblanc, *Phys. Rev. B* **75**, 092406, (2007).
 - [17] B.R. Patyal, B.L. Scott, and R.D. Willett, *Phys. Rev. B* **41**, 1657 (1990).
 - [18] B.C. Watson *et al.*, *Phys. Rev. Lett.* **86**, 5168 (2001).
 - [19] T. Lorenz *et al.*, *Phys. Rev. Lett.* **100**, 067208 (2008).
 - [20] F. Anfuso *et al.*, *Phys. Rev. B* **77**, 235113 (2008).
 - [21] M. Klanjsek *et al.*, *Phys. Rev. Lett.* **101**, 137207 (2008).
 - [22] B. Thielemann *et al.*, arXiv:0809.0440v1.
 - [23] B. Thielemann *et al.*, unpublished.
 - [24] M. Troyer, H. Tsunetsugu, and D. Würtz, *Phys. Rev. B* **50**, 13515 (1994).
 - [25] K. Totsuka, *Phys. Rev. B* **57**, 3454 (1998); F. Mila, *Eur. Phys. J. B* **6**, 201 (1998).
 - [26] A. E. Feiguin and S. R. White, *Phys. Rev. B* **72**, 220401 (2005).
 - [27] Ch. Rüegg *et al.*, *Phys. Rev. Lett.* **95**, 267201 (2005).
 - [28] M. Jaime *et al.*, *Phys. Rev. Lett.* **93**, 087203 (2004).
 - [29] Y. Maeda, C. Hotta, and M. Oshikawa, *Phys. Rev. Lett.* **99**, 057205 (2007).